

FINITE-TIME CONTROL FOR NONHOLONOMIC MOBILE ROBOT BY BRAIN EMOTIONAL LEARNING-BASED INTELLIGENT CONTROLLER

YINGNAN BIAN^{1,2}, JINZHU PENG^{1,*} AND CHUANG HAN¹

¹School of Electrical Engineering
Zhengzhou University

No. 100, Science Avenue, Zhengzhou 450001, P. R. China

*Corresponding author: jzpeng@zzu.edu.cn

²The Airport Group Limited Company of Henan Province
No. 1, Airport Yingbin Road, Zhengzhou 451161, P. R. China
kg087byn@126.com

Received July 2017; revised November 2017

ABSTRACT. *Considering the modeling uncertainties and external disturbances in the wheeled mobile robot system with nonholonomic constraints, this paper proposes a novel intelligent control method to achieve the tracking control of system in finite time and reduce the chattering phenomenon simultaneously. The proposed intelligent control method combines the brain emotional learning (BEL) method with terminal sliding mode control (TSMC) method, where the uncertainties and nonlinear terms of the system are approximated by using BEL method, and the tracking error can converge to the equilibrium point in finite time by using TSMC method. Based on the Lyapunov stability theory, the closed-loop control system is proved to be stable. Finally, compared with the conventional method, the simulation results show that the proposed BEL-based TSMC can reduce the chattering phenomenon better. Moreover, the tracking error of the system can converge to the equilibrium point in finite time.*

Keywords: Brain emotional learning, Terminal sliding mode control, Mobile robot, Nonholonomic constraints

1. Introduction. To control the challenging mobile robot systems nonholonomic constraints, which are not integratable and cannot be written as time derivatives of some functions of the generalized co-ordinates, various control methods have been applied during the past decades [1, 2, 3, 4]. Peng and Shi [1] developed smooth static time invariant state feedback for a velocity-controlled mobile robot with nonholonomic constraint. In [2, 3], the backstepping technique was used to design the adaptive and robust controllers for the nonholonomic systems.

Sliding mode control (SMC), which is also named as variable structure control, has been widely used in the nonlinear system due to its strong robustness. When the sliding mode control method is employed for tracking control of nonholonomic mobile robot, the modeling uncertainties and external disturbances can be effectively eliminated and reduced [5, 6]. Slotine and Li [5] proposed a robust sliding mode tracking controller for nonholonomic mobile robots. In recent years, many scholars have integrated various intelligent methods into SMC for tracking control of the mobile robot. Park et al. [7] proposed an adaptive neural sliding mode control method for trajectory tracking of nonholonomic wheeled mobile robots with model uncertainties and external disturbances. By combining the time delay control with the sliding mode control, Roy et al. [8] designed a time delay sliding control and the hybrid method can eliminate the individual shortcomings while

retaining the positive advantages. Based on weighted integral gain rate, Niu et al. [9] presented a novel SMC, which is applied to the spray mobile robot in the complex unknown environment. The above literature can effectively reduce the chattering phenomenon; however, the errors of the system cannot be converged to the equilibrium point in finite time. Therefore, it cannot be applied for tracking control of the mobile robot that need high precision directly.

Terminal sliding mode control (TSMC) [10] was proposed to achieve the equilibrium point convergence in finite time. Considering singularity in the system, Masood [11] presented a TSMC which makes the states of the system converge in finite time. Moreover, the effectiveness of the proposed algorithm is verified in a practical wheeled mobile robot. Zhang et al. [12] designed the global finite-time control law for the angular velocity, then the advance velocity control law was designed by using TSMC, and the stability of the system can be guaranteed and the effectiveness was verified by a wheeled mobile robot. Xin et al. [13] employed a dynamic model of a wheeled mobile robot and took the motor torque as the control input and a continuous finite-time control method was employed to design a tracking controller. Li and Geng [14] proposed a sliding mode controller at torques level such that both the position and the orientation tracking errors converge to zero in finite time. Wu et al. [15] presented a finite-time control strategy for a general class of nonholonomic dynamic systems with unknown virtual control coefficients and system parameters, where the system's dynamic is driven to reach a set of predefined surfaces in finite time. However, the chattering phenomenon in the above finite-time control method still exists. This is because the chattering phenomenon is the inherit characteristics of the SMC and TSMC methods; therefore, most researches proposed various control approaches combining adaptive and/or intelligent methods with the SMC and/or TSMC methods to reduce the chattering as small as possible.

Brain emotional learning (BEL) is an online learning algorithm for emotional neural networks [16]. Based on Moren's theory [17], Lucas et al. [18] developed a BEL-based intelligent control method, which has been widely applied in various fields via generating the appropriate input signals from the relevant signals during the brain emotional learning process. In general, the algorithm was usually used as a controller which is similar to adaptive PID controller [19, 20]. In [21], BEL-based intelligent control was also used for trajectory tracking control of mobile robot and achieved good tracking performance. In this paper, a novel hybrid control method that combines the BEL-based intelligent control with the TSMC is proposed to achieve the finite-time convergence of the tracking error in the system and reduce the chattering phenomenon simultaneously.

The remainder of the paper is organized as follows. In Section 2, the preliminaries including BEL and dynamic characteristics of mobile robot are introduced. In Section 3, the control architecture of mobile robot based on TSMC is presented. Then, the proposed novel hybrid method which combines BEL-based intelligent control with TSMC is conducted in Section 4. Based on Lyapunov theory, the stability of the proposed hybrid method is proven in Section 4. In Section 5, the simulation results show that the proposed control strategy is more effective by comparing with SMC and TSMC. Finally, the conclusions are drawn in Section 6.

2. Problem Statement and Preliminaries.

2.1. Brain emotional learning-based intelligent control. The emotional learning control, named BEL-based intelligent control or brain limbic system (BLS), is inspired by the human's brain. The algorithm is designed by simulating the brain's emotional learning process. The structure of BEL-based intelligent control is shown in Figure 1.

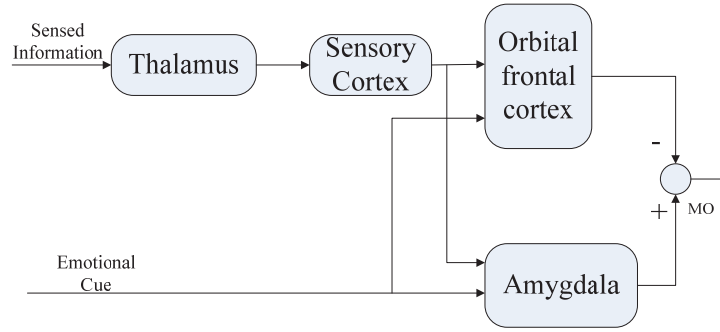


FIGURE 1. The computational model of BEL-based intelligent control

As shown in Figure 1, the BEL-based intelligent control consists of 4 components: thalamus, sensory cortex, orbital frontal cortex and amygdala. The four specified components conduct their respective functions [22]. In general, two stages of learning and signal processing would usually occur during an emotional stimulus and response. The BEL-based intelligent control contains two input signals: sensed information (SI) and emotional cue (EC), and one output signal MO , which is defined as the sum of the two outputs of the amygdala and orbitofrontal cortex, and has the form,

$$MO = \sum_j A_j - \sum_j OC_j \quad (1)$$

where A is the output of the amygdala; OC denotes the output of the orbitofrontal cortex; j is the number of the nodes in the amygdala and the orbitofrontal cortex. The process of emotional learning is divided into two parts: the learning process of the amygdala and the learning process of the orbitofrontal cortex.

2.1.1. *The learning process of amygdala.* Whenever the stimulus signals (SI and EC) entered into the BEL-based intelligent control, there is a corresponding node in the amygdala receiving it. If the sensory input has j stimulus signals, the output of each node corresponding in the amygdala can be described as follows,

$$A_j = G_{A_j} SI_j \quad (2)$$

where G_{A_j} is the weight of the node A_j . The learning process of amygdala is the process of adjusting the weight of each node dynamically. Based on associative learning method, the updating law of the weight G_{A_j} is given as follows,

$$\Delta G_{A_j} = \Gamma SI_j \max \left\{ 0, EC_j - \sum_j A_j \right\} \quad (3)$$

where Γ denotes the learning rate, which is a constant between 0 and 1.

2.1.2. *The learning process of orbitofrontal cortex.* Whenever a stimulus signal entered into the BEL-based intelligent control, there is also a corresponding node in the orbitofrontal cortex receiving it. The stimulus signals are SI and EC , while the output is MO . The output of each node in the orbitofrontal cortex has the following form with,

$$OC_j = G_{OC_j} SI_j \quad (4)$$

where G_{OC_j} is the weight of the node OC_j . The updating law of the weight G_{OC_j} is given as follows,

$$\Delta G_{OC_j} = \Upsilon SI_j (MO - EC_j) \quad (5)$$

where Υ denotes the learning rate, and it is a tiny positive number. In general, Υ is smaller than Γ . The choice of learning rate of emotional learning algorithm is usually based on experience and it has a great influence on the output of the model. Based on the difference between the *EC* and the output signal *MO*, the output value of the frontal cortex is adjusted adaptively to stimulate or suppress the output of the amygdala. After a period of learning time, the output *MO* can approximate the *EC*.

2.2. Dynamic characteristics of wheeled robot. In general, a two-wheeled driven mobile robot is shown Figure 2. The mobile robot is composed of two coaxial driven wheels and an auxiliary guiding wheel. The power sources of the two driven wheels are derived from the drive motors respectively. In Figure 2, r is the radius of the two driven wheels; R is half of the distance between the two driven wheels.

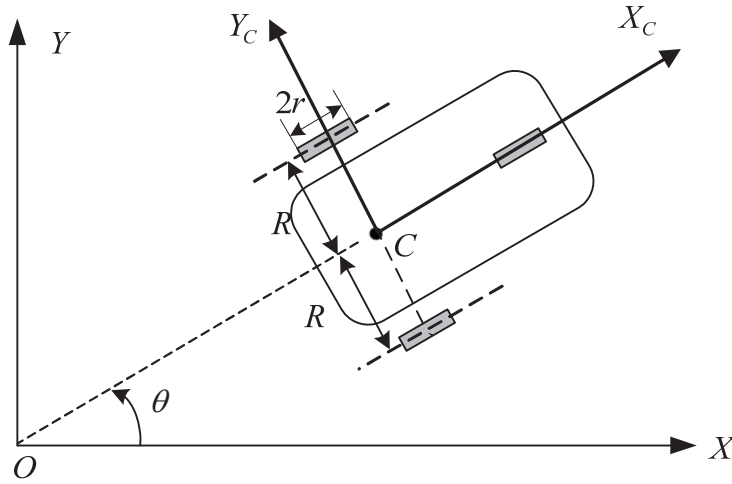


FIGURE 2. The two-wheeled driven mobile robot

Considering the modeling uncertainties and external disturbances, the dynamic characteristics of the mobile robot with nonholonomic constraints can be described as follows [23],

$$M(q)\ddot{q} + C(q, \dot{q})\dot{q} + G(q) + \tau_d = B(q)\tau - A^T(q)\lambda \tag{6}$$

$$A(q)\dot{q} = 0 \tag{7}$$

where $q = [x, y, \theta]^T$, x and y represent the positions of the mobile robot in the X axis and Y axis respectively, and θ denotes the angle between the forward direction of the robot and X axis; $M(q) \in \mathbb{R}^{3 \times 3}$ denotes the symmetric and positive definite inertia matrix; $C(q, \dot{q}) \in \mathbb{R}^{3 \times 3}$ is the Coriolis force matrix; $G(q) \in \mathbb{R}^{3 \times 1}$ is the gravity matrix; $\tau_d \in \mathbb{R}^{3 \times 1}$ is the external disturbance; $B(q) \in \mathbb{R}^{3 \times 2}$ is the input transformation matrix, $\tau \in \mathbb{R}^{2 \times 1}$ is the torque input vector, $A(q) \in \mathbb{R}^{1 \times 2}$ denotes the constraint matrix, and λ is the constraint force. Equation (7) represents the nonholonomic constraints of the mobile robot system.

Selecting a full rank matrix $J(q)$, then Equation (6) can be simplified as follows,

$$\bar{M}(q)\ddot{Z} + \bar{C}(q, \dot{q})\dot{Z} + \bar{G}(q) + \bar{\tau}_d = \bar{\tau} \tag{8}$$

$$\dot{q} = J(q)\dot{Z} \tag{9}$$

where

$$J(q) = \begin{bmatrix} \cos \theta & \sin \theta & 0 \\ 0 & 0 & 1 \end{bmatrix}^T \tag{10}$$

$$\dot{Z} = V = [v \ w]^T \quad (11)$$

where v and w represent the linear velocity and angular velocity of the mobile robot, respectively. Considering that the actual system has modeling uncertainties, the parameter matrices $\bar{M}(q)$, $\bar{C}(q, \dot{q})$ and $\bar{G}(q)$ can be separated as nominal parts denoted by $\bar{M}_0(q)$, $\bar{C}_0(q, \dot{q})$ and $\bar{G}_0(q)$, and the uncertain parts denoted by $\Delta\bar{M}(q)$, $\Delta\bar{C}(q, \dot{q})$ and $\Delta\bar{G}(q)$, respectively. Furthermore, these variables satisfy the following relationships,

$$\begin{cases} \bar{M}(q) = \bar{M}_0(q) + \Delta\bar{M}(q) \\ \bar{C}(q, \dot{q}) = \bar{C}_0(q, \dot{q}) + \Delta\bar{C}(q, \dot{q}) \\ \bar{G}(q) = \bar{G}_0(q) + \Delta\bar{G}(q) \end{cases} \quad (12)$$

Then Equation (8) can be calculated further as follows,

$$\bar{M}_0(q)\ddot{Z} + \bar{C}_0(q, \dot{q})\dot{Z} + \kappa = \bar{\tau} \quad (13)$$

where $\kappa = \Delta\bar{M}(q)\ddot{Z} + \Delta\bar{C}(q, \dot{q})\dot{Z} + \Delta\bar{G}(q) + \bar{\tau}_d$.

Property 2.1. *The nominal inertia matrix $\bar{M}_0(q)$ is symmetric and positive definite.*

Assumption 2.1. *The uncertainties and external disturbances in Equation (13) are bounded, which means that κ is bounded and satisfies,*

$$\|\kappa\| \leq D_\kappa \quad (14)$$

where D_κ is a positive constant.

Remark 2.1. *Assumption 2.1 is reasonable, since the uncertain parts $\Delta\bar{M}(q)$, $\Delta\bar{C}(q, \dot{q})$ and the external disturbance $\bar{\tau}_d$ are usually assumed to be bounded. Besides, the signals \ddot{Z} and \dot{Z} are also bounded.*

Assumed that the reference trajectory is described as $q_r = [x_r, y_r, \theta_r]^T$ and $V_r = [v_r, w_r]^T$. Then the tracking error of the mobile robot can be defined as follows,

$$e_q = \begin{bmatrix} e_1 \\ e_2 \\ e_3 \end{bmatrix} = \begin{bmatrix} \cos \theta & \sin \theta & 0 \\ -\sin \theta & \cos \theta & 0 \\ 0 & 0 & 1 \end{bmatrix} \quad (15)$$

Theorem 2.1. [19] *The velocity control law V_d is designed as follows,*

$$V_d = \begin{bmatrix} k_1 e_1 + v_r \cos e_3 \\ w_r + k_2 e_2 v_r + k_3 v_3 \sin e_3 \end{bmatrix} \quad (16)$$

where $k_1 > 0$, $k_2 > 0$, $k_3 > 0$ are the controller gains. Then, the theoretical stability with respect to the reference trajectory can be achieved.

Definition 2.1. *Define the variable $\dot{Z}_d = V_d$. The research on the trajectory tracking for the mobile robot will be based on the error signal e , and it has the following form,*

$$e = Z_d - Z \quad (17)$$

3. TSMC Method for Noholonomic Mobile Robot. For Equations (8) and (9), the trajectory tracking control for nonholonomic mobile robot will be designed based on TSMC method, and the sliding surface can be described as follows,

$$s = \dot{e} + l e^{\frac{\alpha}{\beta}} \quad (18)$$

where l denotes a diagonal gain matrix, and α and β ($\beta > \alpha$) are positive odds.

Theorem 3.1. *Considering the dynamic Equations (8) and (9) of the mobile robot that contain modeling uncertainties and external disturbances, suppose that Assumption 2.1 is satisfied. Then the TSMC controller can be designed as follows,*

$$\bar{\tau} = \bar{\tau}_0 + \bar{\tau}_s \quad (19)$$

where

$$\bar{\tau}_0 = \bar{M}_0(q) \left(\ddot{Z}_d + K_p s + \frac{\alpha}{\beta} l e^{\alpha/\beta-1} \dot{e} \right) + \bar{C}_0(q, \dot{q}) \dot{Z} \quad (20)$$

$$\bar{\tau}_s = \rho \operatorname{sgn}(s) \quad (21)$$

where K_p is a positive diagonal gain matrix. ρ is selected with the condition that $\rho > D_\kappa$. Then the controller can guarantee that all the state variables of the closed-loop system are bounded.

Proof: Let us select the Lyapunov function:

$$L = \frac{1}{2} s^T s \quad (22)$$

Differentiating the above equation yields,

$$\dot{L} = s^T \dot{s} = s^T \left(\ddot{e} + l \frac{\alpha}{\beta} e^{\alpha/\beta-1} \dot{e} \right) \quad (23)$$

Considering $\ddot{e} = \ddot{Z}_d - \ddot{Z}$, then substituting Equations (19)-(21) into Equation (13) yields,

$$\ddot{e} = -K_p s - l \frac{\alpha}{\beta} e^{\alpha/\beta-1} \dot{e} + \bar{M}_0^{-1}(q) (\kappa - \rho \operatorname{sgn}(s)) \quad (24)$$

Substituting Equation (24) into Equation (23), we obtain,

$$\begin{aligned} \dot{L} &= s^T \left[-K_p s + \bar{M}_0^{-1}(q) (\kappa - \rho \operatorname{sgn}(s)) \right] \\ &= -s^T K_p s - s^T \bar{M}_0^{-1}(q) (\rho \operatorname{sgn}(s) - \kappa) \\ &\leq 0 \end{aligned} \quad (25)$$

As a result, the closed-loop system is then stable. Moreover, the error of the system can converge to the equilibrium point in finite time since that the nonlinear term is introduced into the sliding surface.

Remark 3.1. *According to Remark 2.1, the parameters \ddot{Z} and \dot{Z} are bounded. However, the specified upper bound values are usually difficult to acquire accurately. As a result, the upper bound D_κ is also uncertain. Then the parameter ρ of the controller should be chosen as large as possible.*

4. The Proposed Hybrid Control Method. Although the TSMC method can achieve good tracking performance, there still exists chattering phenomenon. To reduce the chattering more effectively and achieve the finite-time convergence, the BEL-based intelligent control method is employed to approximate the nonlinear term of the system. The novel hybrid method which combines BEL-based intelligent control with TSMC is then designed.

Assumption 4.1. *Supposed that only the nominal parameter of the inertia matrix $\bar{M}_0(q)$ is known and the other nominal parameters $\bar{C}_0(q, \dot{q})$ and $\bar{G}_0(q)$ are both assumed to be unknown.*

Remark 4.1. *Assumption 4.1 can be satisfied, since in reality the inertia matrix of a mobile robot is relatively easy to obtain an acceptable precision; furthermore, the parametric uncertainty of inertia matrix is considered.*

Then Equation (6) can be deduced as follows,

$$\bar{M}_0(q)\ddot{Z} + f = \bar{\tau} \quad (26)$$

where $f = \Delta\bar{M}(q)\ddot{Z} + \bar{C}(q, \dot{q})\dot{Z} + \bar{G}(q) + \bar{\tau}_d$.

Assumption 4.2. *The BEL-based intelligent control method is used to approximate the nonlinear terms f , which consists of uncertainties and external disturbances. The output of the BEL-based intelligent control can be described with $MO = \hat{f}$. And the approximation error is derived as,*

$$\|f - MO\| = \|f - \hat{f}\| \leq \varepsilon < D_\kappa \quad (27)$$

where ε is the upper bound of the approximation error and D_κ is the bound of the nonlinear term κ referred in Assumption 2.1.

Remark 4.2. *Assumption 4.2 can be ensured. After a learning period, the output MO of the BEL-based intelligent control method can approximate EC . As a result, Equation (27) can be satisfied when the EC signal is equal to f and the parameters of the BEL-based intelligent control method are set up based on experience properly.*

Theorem 4.1. *For the dynamic Equations (8) and (9), supposed that Assumptions 2.1, 4.1 and 4.2 are satisfied, the terminal sliding surface is chosen as Equation (18). Then, the hybrid control law based on BEL-based intelligent control and TSMC is designed as follows,*

$$\bar{\tau} = \bar{\tau}_0 + \bar{\tau}_s + \bar{\tau}_p \quad (28)$$

where the equivalent control input $\bar{\tau}_0$ has the following form,

$$\bar{\tau}_0 = \bar{M}_0(q) \left(\ddot{Z}_d + K_p s + \frac{\alpha}{\beta} l e^{\alpha/\beta-1} \dot{e} \right) \quad (29)$$

Then $\bar{\tau}_s$ is designed as follows,

$$\bar{\tau}_s = \rho_0 \text{sgn}(s) \quad (30)$$

where ρ_0 is a positive constant. The control input $\bar{\tau}_p$ is equal to the output (MO) of the BEL-based intelligent control method,

$$\bar{\tau}_p = MO = \sum_j A_j - \sum_j OC_j \quad (31)$$

where the detail parameters of the BEL-based intelligent control are described as follows,

$$SI = [\mu_1 e \quad \mu_2 \dot{e}]^T \quad (32)$$

$$EC = \bar{\tau} - \bar{M}_0(q)\ddot{Z} \quad (33)$$

where $0 < \mu_1 < 1$, $0 < \mu_2 < 1$ are defined by user.

Guarantee that (i) the closed-loop system is stable and the chattering phenomena can be reduced more effectively than the TSMC method and (ii) the error of the system can be converged to the equilibrium point in the t_s :

$$t_s = \frac{\beta}{l(\beta - \alpha)} \|e(0)\|^{1-\alpha/\beta} \quad (34)$$

Proof: Let us define the Lyapunov function:

$$L = \frac{1}{2}s^T s \tag{35}$$

Considering the relationship $\ddot{e} = \ddot{Z}_d - \ddot{Z}$, and substituting Equations (27)-(30) into Equation (26), we obtain,

$$\begin{aligned} \dot{L} &= s^T \dot{s} = s^T \left(\ddot{e} + l \frac{\alpha}{\beta} e^{\alpha/\beta-1} \dot{e} \right) \\ &= s^T \left[-K_p s - l \frac{\alpha}{\beta} e^{\alpha/\beta-1} \dot{e} + \bar{M}_0^{-1}(q) (f - MO - \rho_0 \text{sgn}(s)) + l \frac{\alpha}{\beta} e^{\alpha/\beta-1} \dot{e} \right] \\ &= s^T [-K_p s + \bar{M}_0^{-1}(q) (f - MO - \rho_0 \text{sgn}(s))] \\ &= -s^T K_p s - s^T \bar{M}_0^{-1}(q) [\rho_0 \text{sgn}(s) - (f - MO)] \end{aligned} \tag{36}$$

Taking Assumption 4.2 into account, we can select $\rho_0 \geq \varepsilon$ and then we have,

$$\dot{L} \leq 0 \tag{37}$$

As a result, the stability of the closed-loop system is proven. Moreover, according to Assumption 4.2 and comparing Equation (21) with Equation (30), the value of ρ_0 can be chosen smaller than ρ , and the smaller gain of sign function generally leads to the smaller chattering phenomenon of TSMC. Therefore, the goal of reducing the chattering phenomenon more effectively than TSMC method can be achieved. Considering the TSMC sliding surface described by Equation (18), we obtain,

$$dt = -\frac{1}{l} e^{-\alpha/\beta} de \tag{38}$$

Integrating Equations (37) and (38) yields,

$$\int_0^t dt = \int_{e(0)}^0 -\frac{1}{l} e^{-\alpha/\beta} de \tag{39}$$

As a result, the time variable t_s , which describes that the state of the system converges to the equilibrium point from the sliding surface, has the form with

$$t_s = \frac{\beta}{l(\beta - \alpha)} \|e(0)\|^{1-\alpha/\beta} \tag{40}$$

where $e(0) \neq 0$ denotes the initial error of the system.

According to the above analysis, the architecture of the closed-loop system is shown in Figure 3.

Remark 4.3. Note that the sign function is introduced in Equation (30), the application of such control signals to the robotic system can still result in chattering caused by the signal discontinuity. To reduce the chattering problem further, the control law $\bar{\tau}_s$ is replaced by the following forms,

$$\bar{\tau}_s = \begin{cases} \frac{\rho_0 (s^T \bar{M}_0^{-1}(q))^T \|s\| \|\bar{M}_0^{-1}(q)\|}{\|s^T \bar{M}_0^{-1}(q)\|^2}, & \|s^T \bar{M}_0^{-1}(q)\| \geq \eta \\ \frac{\rho_0 (s^T \bar{M}_0^{-1}(q))^T \|s\| \|\bar{M}_0^{-1}(q)\|}{\eta^2}, & \|s^T \bar{M}_0^{-1}(q)\| < \eta \end{cases} \tag{41}$$

where the value η is enough small and satisfies that $\|s^T \bar{M}_0^{-1}(q)\| \approx \eta$ is correct when $\|s^T \bar{M}_0^{-1}(q)\| < \eta$.

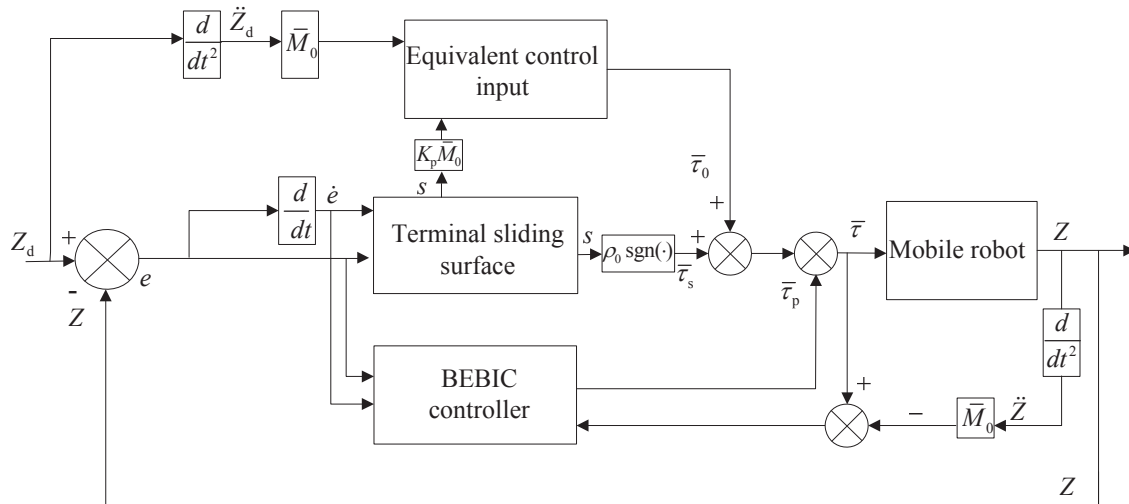


FIGURE 3. The architecture of the proposed hybrid method

Remark 4.4. It is easily seen that the increase in the control gain K_p and ρ_0 will result in a better tracking performance and quicker convergence. However, for Equations (29) and (30), it is not recommended to use very large positive design parameters K_p and ρ_0 , since this may lead to a high gain control and increase the chattering of the closed-loop system due to the sign function. Therefore, the parameters should be adjusted carefully for achieving suitable performance and control action.

5. Numerical Examples. The effectiveness of the proposed hybrid method is verified in comparison with the SMC and TSMC method under the same conditions. The specified parameters of the mobile robot are given as $m = 10\text{kg}$, $I = 5\text{kg}\cdot\text{m}^2$, $R = 0.25\text{m}$, $r = 0.05\text{m}$. The parameters are chosen as $k_1 = 8$, $k_2 = 6.3$, $k_3 = 4.2$.

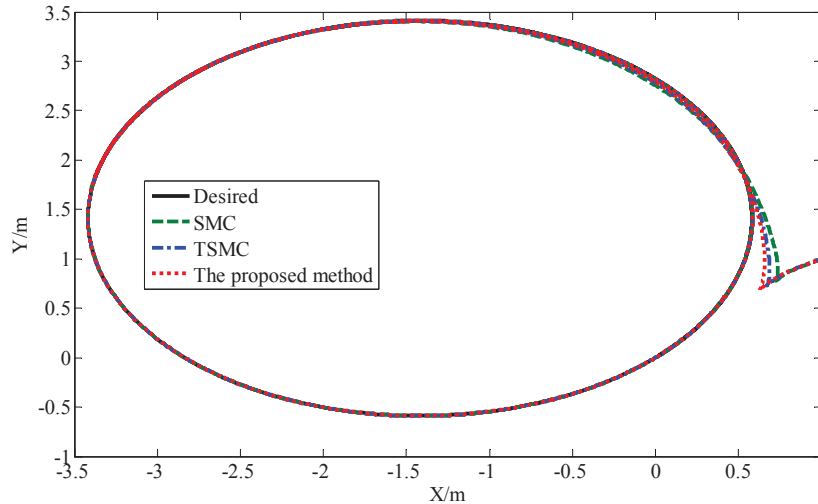
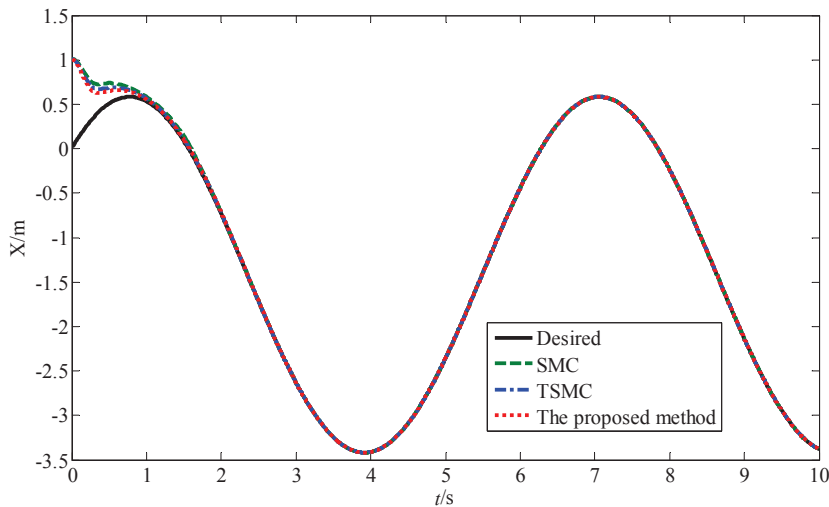
The gain matrix K_r in the SMC is chosen as $K_r = 60I_{2\times 2}$. The relevant parameters of the TSMC are chosen as: $\rho = 60$, $K_p = 4I_{2\times 2}$. The parameters of the terminal sliding surface are $\alpha = 3$, $\beta = 5$.

The parameters of the adaptive control input $\bar{\tau}_p$ in the proposed controller are chosen as: $\mu_1 = 0.3$, $\mu_2 = 0.4$, $\Gamma = 0.15$, $\Upsilon = 0.03$. The parameters of the equivalent control input are chosen as the same as TSMC method; the parameters of the control input $\bar{\tau}_s$ are set up with $\rho_0 = 50$, $\eta = 0.01$. The parameter l of the sliding surface among the three methods is selected as the same value $l = 5I_{2\times 2}$.

Assumed that the desired trajectory is a circle and the desired velocity of mobile robot is $V_r = [2, 1]^T$. The initial value of the desired trajectory is $q_r = [0, 0, \pi/4]^T$. The real initial position of the mobile robot is $q(0) = [1, 1, \pi/6]^T$ and the real initial velocity is $V(0) = [0.5, 0.5]^T$. The specific simulation results are shown in Figures 4-10.

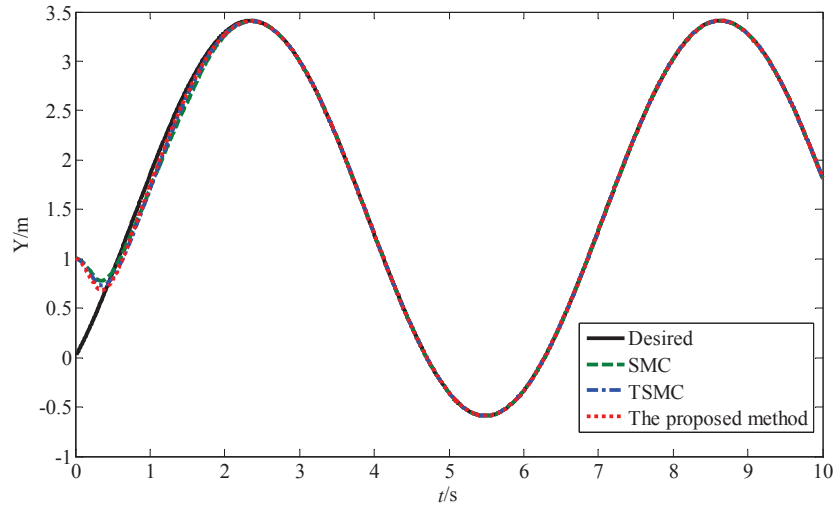
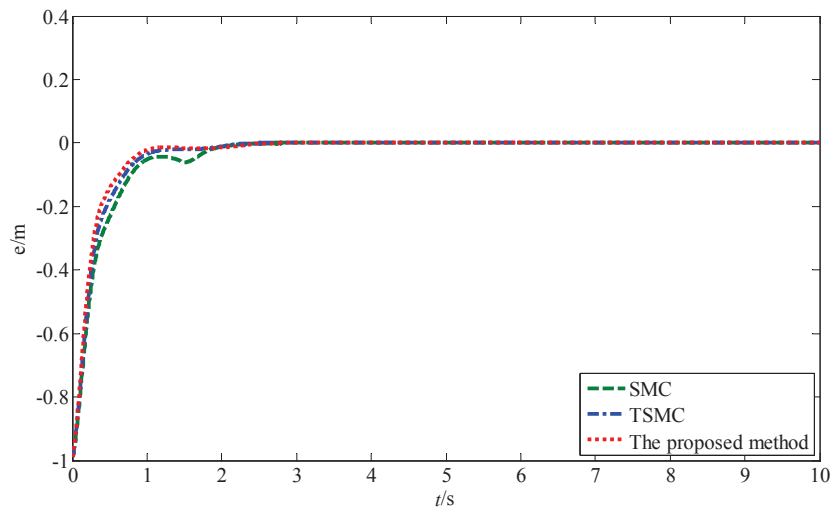
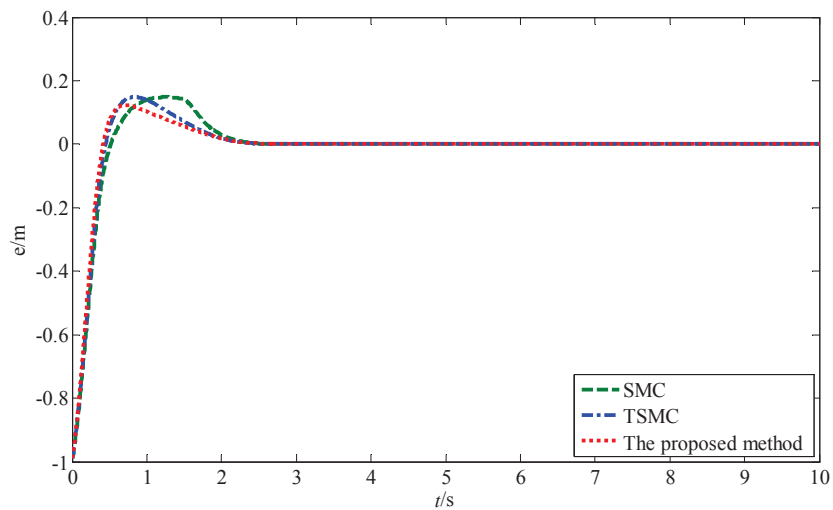
Under the same modeling uncertainties and external disturbance, Figure 4 shows the results for tracking a circle by using SMC, TSMC and the proposed hybrid method respectively. Figure 5 and Figure 6 are the tracking trajectories in the X axis and Y axis directions respectively. The tracking errors in the X axis and the Y axis directions are shown in Figure 7 and Figure 8, respectively. Figure 9 and Figure 10 are the control torques of the left and right wheels, respectively.

It can be seen that the proposed hybrid method can achieve the desired trajectory in a finite time and can greatly reduce the chattering phenomenon of the control torque compared with SMC. In addition, compared with the TSMC, it can be also easily seen that the convergence time and tracking errors of the proposed method are nearly as the

FIGURE 4. The tracking trajectories on the X - Y planeFIGURE 5. The tracking trajectories in the X axis

same as the TSMC method due to the same parameter of the terminal sliding surface. However, the chattering phenomenon of the control torques of two wheels can be reduced more effectively than the TSMC method. The simulation results thus demonstrate that the proposed BEL-based intelligent robust hybrid tracking control method can effectively control the nonholonomic mobile robot with uncertainties and disturbances.

6. Conclusions. This paper proposed a novel robust hybrid method which combined BEL-based intelligent controller with TSMC method, which is applied to tracking control for mobile robots with nonholonomic constraints. Based on the Lyapunov theory, the stability of the system can be guaranteed. Moreover, the proposed method can make the tracking errors converge to zeros in a finite time and reduce the chattering phenomenon of the control torque at the same time. Finally, under the same external disturbance and the modeling uncertainties, the simulation tests were drawn by using SMC, TSMC and the proposed method respectively, and the results show that the proposed BEL-based intelligent robust hybrid control method demonstrated better robust and effective

FIGURE 6. The tracking trajectories in the Y axisFIGURE 7. The tracking errors in the X axisFIGURE 8. The tracking errors in the Y axis

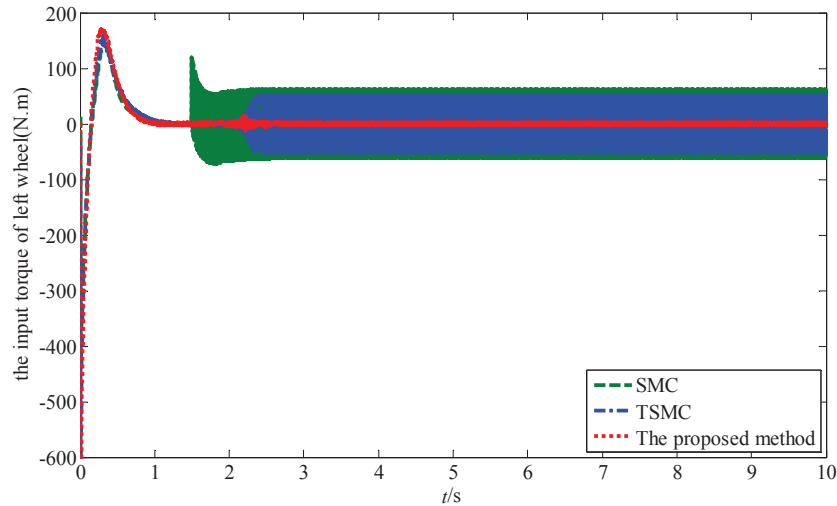


FIGURE 9. The input torques of the left wheel

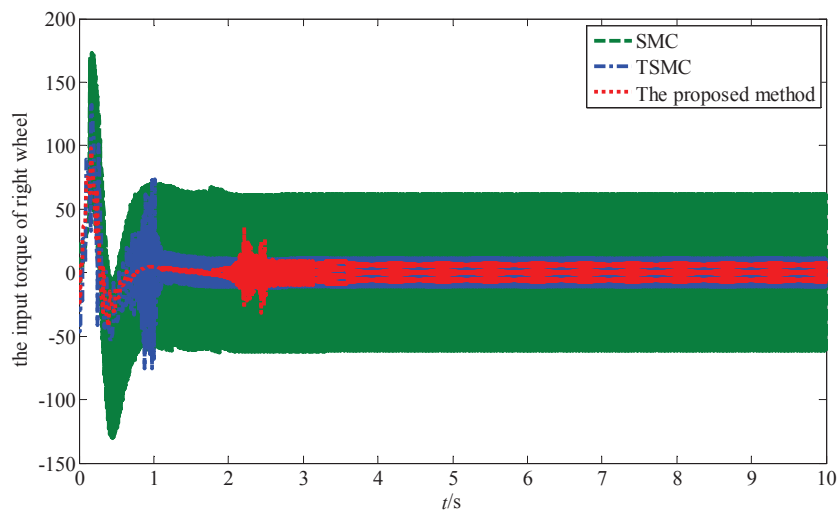


FIGURE 10. The output torques of the right wheel

control performance on nonholonomic mobile robot in comparison with SMC and TSMC approaches. As future work, the proposed BEL-based intelligent TSMC approach will be proven experimentally and applied to other kinds of electromechanical systems.

Acknowledgment. This work is partially supported by the National Natural Science Foundation of China (61773351 and 61473265), Natural Science Foundation of Henan Province (162300410260) and Outstanding Young Teacher Development Fund of Zhengzhou University (1521319025). The authors also gratefully acknowledge the helpful comments and suggestions of the reviewers, which have improved the presentation.

REFERENCES

- [1] S. Peng and W. Shi, Adaptive fuzzy integral terminal sliding mode control of a nonholonomic wheeled mobile robot, *Mathematical Problems in Engineering*, vol.2017, no.4, pp.1-12, 2017.
- [2] Y. Koubaa, M. Boukattaya and T. Damak, Adaptive sliding-mode control of nonholonomic wheeled mobile robot, *Proc. of International Conference on Sciences and Techniques of Automatic Control and Computer Engineering*, pp.336-342, 2015.

- [3] T. N. Kigezi, S. Alexandru, E. Mugabi et al., Sliding mode control for tracking of nonholonomic wheeled mobile robots, *Proc. of Control Conference*, pp.21-26, 2015.
- [4] Z. P. Wang, W. R. Yang and G. X. Ding, Sliding mode control for trajectory tracking of nonholonomic wheeled mobile robots based on neural dynamic model, *Proc. of the 2nd WRI Global Congress on Intelligent Systems*, pp.270-273, 2010.
- [5] J. J. E. Slotine and W. Li, *Applied Nonlinear Control*, China Machine Press, 2004.
- [6] Y. Boutalis, D. Theodoridis, T. Kottas et al., *System Identification and Adaptive Control*, Springer International Publishing, 2014.
- [7] B. S. Park, S. J. Yoo, B. P. Jin et al., Adaptive neural sliding mode control of nonholonomic wheeled mobile robots with model uncertainty, *IEEE Trans. Control Systems Technology*, vol.17, no.1, pp.207-214, 2009.
- [8] S. Roy, S. Nandy, R. Ray et al., Time delay sliding mode control of nonholonomic wheeled mobile robot: Experimental validation, *Proc. of IEEE International Conference on Robotics and Automation*, pp.2886-2892, 2014.
- [9] X. M. Niu, G. Q. Gao and H. Y. Zhou, Sliding mode path tracking control for spraying mobile robots based on weighed integral gain reaching law, *Applied Mechanics & Materials*, vol.313, no.2, pp.932-936, 2013.
- [10] J. Xia, Research and development of terminal sliding mode control method, *Chemical Automation and Instrumentation*, vol.38, no.9, pp.1043-1047, 2011.
- [11] G. Masood, Finite-time tracking using sliding mode control, *Journal of the Franklin Institute*, vol.351, no.5, pp.2966-2990, 2014.
- [12] Y. Zhang, G. Liu and B. Luo, Finite-time cascaded tracking control approach for mobile robots, *Information Sciences*, vol.284, no.1, pp.31-43, 2014.
- [13] L. Xin, Q. Wang, J. She et al., Robust adaptive tracking control of wheeled mobile robot, *Robotics and Autonomous Systems*, vol.78, pp.36-48, 2016.
- [14] X. Li and Z. Geng, Adaptive sliding mode tracking control for nonholonomic wheeled mobile robots with finite time convergence, *The 36th Chinese Control Conference (CCC)*, pp.720-725, 2017.
- [15] Y. Q. Wu, C. L. Zhu and Z. C. Zhang, Finite time stabilization of a general class of nonholonomic dynamic systems via terminal sliding mode, *International Journal of Automation and Computing*, vol.13, no.6, pp.585-595, 2016.
- [16] E. Lotfi, O. Khazaei and F. Khazaei, Competitive brain emotional learning, *Neural Processing Letters*, 2017.
- [17] J. Moren, Emotion and learning: A computational model of the amygdala, *Cybernetics and Systems: An International Journal*, vol.32, no.6, pp.611-636, 2001.
- [18] C. Lucas, D. Shahmirzadi and N. Sheikholeslami, Introducing BELBIC: Brain emotional learning based intelligent controller, *Intelligent Automation & Soft Computing*, vol.10, no.1, pp.11-21, 2004.
- [19] M. A. Sharbafi, C. Lucas and R. Daneshvar, Motion control of omni-directional three-wheel robots by brain-emotional-learning-based intelligent controller, *IEEE Trans. Systems Man & Cybernetics: Part C*, vol.40, no.6, pp.630-638, 2010.
- [20] R. Mohammadi-Milasi, C. Lucas and B. Nadjar-Arrabi, Speed control of an interior permanent magnet synchronous motor using BELBIC (brain emotional learning based intelligent controller), *Proc. of Automation Congress*, pp.280-286, 2005.
- [21] C. Kim and R. Langari, A mobile robot target tracking via brain limbic system based control, *International Journal of Robotics and Automation*, vol.26, no.3, pp.288-295, 2011.
- [22] H. Yi and R. Langari, A design and bio-inspired control of a novel redundant manipulator with MDOFs links, *International Journal of Robotics and Automation*, vol.27, no.4, pp.422-430, 2012.
- [23] J. Peng, J. Yu and J. Wang, Robust adaptive tracking control for nonholonomic mobile manipulator with uncertainties, *ISA Transactions*, vol.53, no.4, pp.1035-1043, 2014.